Hindawi
Advances in Civil Engineering
Volume 2018, Article ID 7242936, 9 pages
https://doi.org/10.1155/2018/7242936

Research Article

An Enhanced Generalized Plasticity Model for Coarse Granular Material considering Particle Breakage

W. J. Cen,[1] **J. R. Luo**,[1] **W. D. Zhang**,[2] **and M. S. Rahman**[3]

[1]*College of Water Conservancy and Hydropower Engineering, Hohai University, Nanjing 210098, China*
[2]*Hunan Hydro & Power Design Institute, Changsha 410021, China*
[3]*Department of Civil, Construction, and Environmental Engineering, North Carolina State University, Raleigh, NC, USA*

Correspondence should be addressed to W. J. Cen; hhucwj@163.com

Received 8 June 2018; Revised 21 September 2018; Accepted 18 October 2018; Published 15 November 2018

Academic Editor: M. Shahria Alam

In this study, an enhanced constitutive model is developed for coarse granular soil within the framework of generalized plasticity (Pastor, Zienkiewicz, and Chan, 1990). In this model, particle breakage is also considered by introducing the state parameter and the compression index into the plastic modulus, loading vectors, and plastic flow direction vectors of a generalized plasticity model. The calibration of constitutive parameters of the enhanced model is addressed in detail. The numerical simulation of triaxial tests for two types of coarse granular soils under different confining pressures is carried out to illustrate the particle breakage performance of the enhanced model. The good agreement between numerical results and experimental data indicates that the enhanced model can accurately characterize the influence of particle breakage on essential behavior of coarse granular soils.

1. Introduction

Owing to its good compactibility, high shear strength, high hydraulic permeability, and low cost, the rockfill material, as a widely available coarse granular soil, is generally used in earth-rockfill dams. With the sustained breakthrough of dam height to 300 m level, the confining pressure increases sharply, which results in significant particle breakage and compressive deformation for the rockfill material. Therefore, the influence of particle breakage on the essential material behavior under high confining pressure should be considered in constitutive modeling of coarse granular soils.

Over the past few decades, many new or modified constitutive models have been proposed for granular soils. Russell and Khalili [1] established a new bounding surface constitutive model for sands, which works in a wide range of pressures, including those which may cause particle crushing. This is done by defining a uniquely shaped critical state line to capture the three modes of plastic deformation observed across a wide range of stresses, including particle rearrangement, particle crushing, and pseudoelastic deformation. Salim and Indraratna [2] have presented a new constitutive model for coarse granular aggregates involving the effect of particle breakage by establishing a plastic flow rule incorporating the energy consumption. Fernández-Merodo et al. [3] developed an enhanced generalized plasticity that is able to reproduce particle damage phenomena for geomaterials. Based on the concept of the binary medium model, a constitutive model of the rockfill material considering grain crushing, which was conceptualized as the binary medium model consisting of the structural system and the breaking bond, was presented, and the relationship between grain crushing rate and breaking parameter was established by Mi et al. [4]. By introducing the crushing critical stress into the modified Cam-clay model, Sun et al. [5] proposed a practical elastoplastic constitutive model which is suitable for description of soil behavior for a wide range of pressures, including those sufficient to cause particle crushing. Adopting a new hardening parameter with the crushing stress, Yao et al. [6] proposed an elastoplastic constitutive model considering sand crushing. Liu et al. [7] proposed a new critical state line that can reflect the effect of

particle breakage for coarse granular soils. And by introducing a state parameter, a new constitutive model for rockfill was formulated based on the generalized plasticity. By introducing a volumetric strain-dependent and pressure-dependent compression index, Chen et al. [8] proposed an elastoplastic constitutive model considering particle breakage for rockfill within the framework of generalized plasticity.

In this paper, the expressions of the compression curve and the critical state line are unified, and an enhanced version of the generalized plasticity model for coarse granular soil considering particle breakage is being proposed. The numerical simulation of triaxial tests of rockfill materials is carried out to validate the good performance of the enhanced model.

2. State Parameter and Critical State of Soil

Been and Jefferies [9] put forward the concept of the state parameter to reflect the compaction condition of soils. The state parameter ψ that depends on the relative density and confining pressure of soil is expressed as

$$\psi = e - e_{cs}, \tag{1}$$

where e is the current void ratio and e_{cs} is the critical void ratio.

The value of the state parameter $\psi < 0$ means that the soil is in a dense state. When $\psi > 0$, the soil is in a loose state. The greater the value of ψ is, the looser the state of soil is, and vice versa. It is worth noting that the value of ψ is zero in the critical state (Figure 1).

The critical state is a condition where shear failure occurs without change of stress and volume for soil. As for clay, the critical state plot can be regarded as a straight line in the $e - \ln p'$ plane [10]. The pressure-dependent critical void ratio e_{cs} is expressed as

$$e_{cs} = e^{\Gamma} - \lambda \ln p', \tag{2}$$

where λ is the slope of the critical state line in the $e - \ln p'$ plane, e^{Γ} corresponds to the critical void ratio for $\ln p' = 0$, and p' is the mean effective pressure.

The experimental fitting of the critical state line of Toyoura sand [11] shows that the critical state plot of sand is not a straight line in the $e - \ln p'$ plane, whereas it can be approximately depicted as a straight line in the $e - (p'/p_a)^{\xi}$ plane, which is expressed as

$$e_{cs} = e_0 - \lambda \left(\frac{p'}{p_a}\right)^{\xi}, \tag{3}$$

where λ is the slope of the critical state line in the $e - (p'/p_a)^{\xi}$ plane, e_0 corresponds to the void ratio for the mean pressure, $p' = 0$, ξ is a material parameter, and p_a is the atmosphere pressure.

The critical void ratio of soil might be negative when the mean effective pressure p' in Equation (3) increases to a certain value, which is obviously unreasonable. Thus, an enhanced version of critical state line proposed by Cen et al. [12] that can well reflect the nonlinearity of the critical state line for both sand and rockfill in the $e - \ln p'$ plane is used with the following form:

$$e_{cs} = a \exp\left(-b\left(\frac{p'}{p_a}\right)^{c}\right), \tag{4}$$

where a, b, and c are the material parameters.

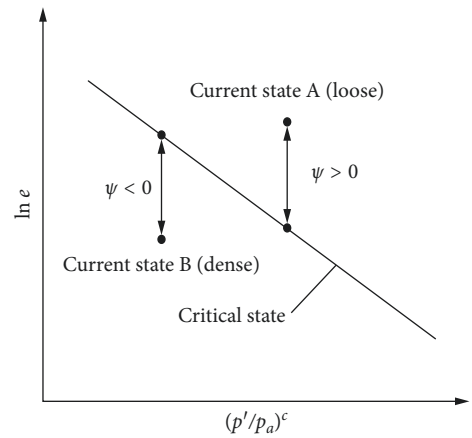

Figure 1: Definition of the state parameter.

A comparison between the critical state lines simulated by Equations (3) and (4) is shown in Figure 2. Both functions fit well with the experimental data from Verdugo and Ishihara [13] under low confining pressures. In consideration of an extrapolation to very high pressures, under which grain crushing becomes dominant, the void ratio obtained with Equation (3) decreases sharply and becomes negative. Conversely, the change rate of the void ratio obtained with Equation (4) reduced when confining pressure increases, which is consistent with deformation characteristics of coarse granular soils. The priority of the form of Equation (4) will be further described in Section 4.3.

3. PZC Generalized Plasticity Model

The theory of generalized plasticity was first introduced by Mróz and Zienkiewicz [14] and later extended by Pastor and Zienkiewicz et al. [15–18]. In contrast to the classical elastoplastic model, the generalized plasticity model by Pastor et al. [17], referred to in the following as the PZC model, has neither an explicitly defined yield surface nor a plastic potential surface and does not need a consistency law to determine the plastic modulus. It provides a relatively simple framework for the prediction of soil mechanical behavior.

In the PZC model, the elastoplastic stiffness tensor $\mathbf{D}^{ep}$ is defined as follows:

$$\mathbf{D}^{ep} = \mathbf{D}^{e} - \frac{\mathbf{D}^{e} : \mathbf{n}_{gL/U} \otimes \mathbf{n} : \mathbf{D}^{e}}{H_{L/U} + \mathbf{n}^{T} : \mathbf{D}^{e} : \mathbf{n}_{gL/U}}, \tag{5}$$

where $\mathbf{D}^{e}$ is the elastic stiffness tensor, $\mathbf{n}$ is the loading direction vector, $\mathbf{n}_{gL/U}$ is the plastic flow direction vector, and $H_{L/U}$ is the loading or unloading plastic modulus. Here, L and U denote the corresponding quantities for loading and unloading, respectively.

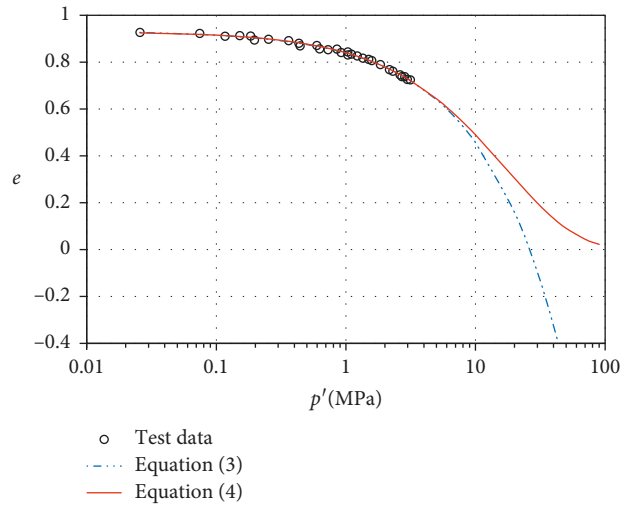

FIGURE 2: Comparison between critical state lines simulated by Equations (3) and (4).

Bulk modulus K and shear modulus G are associated with normalized mean effective stress pressure p'/p_0, where p_0 is the atmospheric pressure, in the following forms:

$$\begin{cases} G = G_{\text{eso}}\left(\dfrac{p'}{p_0}\right), \\ \\ K = K_{\text{evo}}\left(\dfrac{p'}{p_0}\right), \end{cases} \tag{6}$$

where G_{eso} and K_{evo} are reference shear and bulk modulus number, respectively.

The plastic flow direction vector $\mathbf{n}_{\text{g}}$ and the loading direction vector $\mathbf{n}$ are defined as follows:

$$\mathbf{n}_{\text{gL}}^{T} = \frac{1}{\sqrt{1+d_{\text{g}}^2}}\left(d_{\text{g}}, 1\right), \tag{7}$$

$$\mathbf{n}^{T} = \frac{1}{\sqrt{1+d_{\text{f}}^2}}\left(d_{\text{f}}, 1\right). \tag{8}$$

Equations (7) and (8) have the same form only with different variables d_{g} and d_{f}. d_{g} is the dilatancy, on which the plastic flow direction depends, i.e.,

$$d_{\text{g}} = \frac{d\varepsilon_{\text{v}}^{\text{p}}}{d\varepsilon_{\text{s}}^{\text{p}}} = \left(1+\alpha_{\text{g}}\right)\left(M_{\text{g}} - \eta\right), \tag{9}$$

where $d\varepsilon_{\text{v}}^{\text{p}}$ is the plastic volumetric strain, $d\varepsilon_{\text{s}}^{\text{p}}$ is the plastic deviatoric strain, and M_{g} and α_{g} are the material parameters. When $\alpha_{\text{f}} = \alpha_{\text{g}}$ and $M_{\text{f}} = M_{\text{g}}$, the associative flow rule is considered. When $\eta = M_{\text{g}}$, dilatancy $d_{\text{g}} = 0$, and plastic volumetric deformation does not occur, but it does not attain the residual state.

d_{f} is expressed as

$$d_{\text{f}} = \left(1+\alpha_{\text{f}}\right)\left(M_{\text{f}} - \eta\right), \tag{10}$$

where $\eta = q/p'$ is the stress ratio, M_{f} is the stress ratio at failure, and α_{f} is a material parameter.

The plastic modulus H_{L} for loading reads

$$\begin{aligned} H_{\text{L}} &= H_0 p' H_{\text{f}}\{H_{\text{v}} + H_{\text{s}}\}, \\ H_{\text{f}} &= \left(1 - \frac{\eta}{\eta_{\text{f}}}\right)^4, \\ \eta_{\text{f}} &= \left(1 + \frac{1}{\alpha}\right)M_{\text{f}}, \\ \{H_{\text{v}} + H_{\text{s}}\} &= \left(1 - \frac{\eta}{M_{\text{g}}}\right) + \beta_0\beta_1 \exp\left(-\beta_0\xi\right), \\ \xi &= \int \left|d\varepsilon_{\text{s}}^{\text{p}}\right| = \int d\xi, \end{aligned} \tag{11}$$

where H_0 is the plastic modulus number; H_{DM} is a discrete memory factor; H_{f}, H_{v}, and H_{s} are the plastic coefficients; $\eta_{\text{f}} = (1 + 1/\alpha)M_{\text{f}}$ is the stress ratio; $\xi = \int |d\varepsilon_{\text{s}}^{\text{p}}|$ is the accumulated deviatoric plastic strain; and β_0, β_1, α, and γ are material parameters.

For $H_{\text{v}} + H_{\text{s}} > 0\,(H_{\text{L}} > 0)$, hardening of the material occurs, and for $H_{\text{v}} + H_{\text{s}} < 0\,(H_{\text{L}} < 0)$, softening of the material occurs.

4. Proposed Enhanced Model

4.1. Nonlinear Elastic Behavior. In the following, a enhanced generalized plasticity model is proposed where the elastic constitutive tensor is determined by the shear modulus G and bulk modulus K, which, for a more refined modeling, are dependent on both current void ratio e and the normalized pressure $\overline{p}$. In particular, the following empirical equations for G and K are used [13, 19, 20]:

$$\begin{cases} G = G_0 p_{\text{a}} \dfrac{(2.97-e)^2}{1+e}\left(\dfrac{p'}{p_{\text{a}}}\right)^{0.5}, \\ \\ K = K_0 p_{\text{a}} \dfrac{(2.97-e)^2}{1+e}\left(\dfrac{p'}{p_{\text{a}}}\right)^{0.5}, \end{cases} \tag{12}$$

where G_0 is the shear modulus number and K_0 is the bulk modulus number. Equation (12) is also introduced in the modified generalized plasticity models by Ling and Yang [21] and Manzanal et al. [22].

4.2. Dilatancy Equation. According to the dilatancy equation, the plastic flow direction vector $\mathbf{n}_{\text{g}}$ is determined. A widely used dilatancy equation for sand, in which the state parameter ψ is introduced, was proposed by Li et al. [11] in the following form:

$$d_{\text{g}} = \frac{d_0}{M}\left(M\exp\left(m\psi\right) - \eta\right). \tag{13}$$

Equation (13) is not applicable to a coarse granular material, such as rockfill. Liu et al. [23] investigated the dilatancy of rockfill using large-scale triaxial tests and proposed a dilatancy equation for rockfill considering the state parameter ψ. The dilatancy equation is expressed as

$$\zeta = \zeta_0 \left[\exp\left(m_g \psi\right) - \left(\frac{\eta}{M_g}\right)^n \right], \tag{14}$$

where M_g is the critical stress ratio and ζ_0, m, and n are the material parameters. For $n = 1$, Equation (14) is equivalent to Equation (13). Equation (14) can be employed for both fine granular soil and coarse granular soil, e.g., sand and rockfill.

4.3. Compression Index. By using the compression curve proposed by Bauer [24, 25], Chen et al [8] derived a compression index that can reflect the particle breakage of coarse granular soil under high confining pressure. The compression curve proposed by Bauer is expressed by Equation (15), and it can be depicted in the $e - \ln p'$ plane as shown in Figure 3:

$$e = e_0 \exp\left(-\left(\frac{p'}{h_s}\right)^n\right), \tag{15}$$

where e_0 is the initial void ratio of the coarse granular material and h_s is the solid hardness which represents the compliance of the coarse granular depending on the pressure level. The greater the value of h_s is, the less likely the coarse granular material is to be crushed.

As shown in Figure 3, the compression index λ is defined as the slope of the compression curve. If the particle size of clay is well graded, particle breakage will not occur. Under low confining pressure, almost no particle breakage occurs. Thus, the compression curve is approximately linear, and the compression index λ basically remains constant. With increasing confining pressure, particle breakage occurs, the compression curve starts to bend, and the compression index λ starts to increase. When particle breakage is almost done, the grain composition of the soil returns to stability, the compression curve becomes linear again, and the compression index λ also basically remains constant. Thus, the variation of the compression index can represent the particle breakage degree of soil; i.e., the faster the compression index changes, the more significant the particle breakage is, and vice versa. When the compression index λ tends to be constant, the particle breakage will not occur any more.

It can be found that the relationship (15) is similar to the relationship (4) proposed in this paper for modeling the critical state line. By comparison, the parameters a and b in Equation (4) can be related to the initial void ratio e_0 and the solid hardness h_s in Equation (15), respectively. With the concept of the compression index, a new compression index can be obtained from the derivation of the pressure-dependent critical void ratio e_{cs} of the critical state line (Equation (4)) with respect to $\ln p'$:

$$\lambda = \left| \frac{de_{cs}}{d\left(\ln p'\right)} \right| = bc \cdot e \left(\frac{p'}{p_a}\right)^c, \tag{16}$$

where λ is the compression index that represents the particle breakage of coarse granular soil.

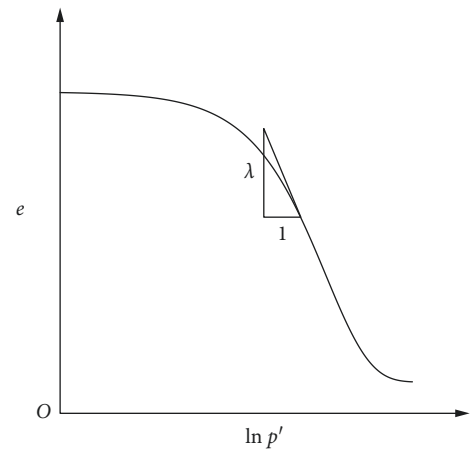

Figure 3: The compression curve of soil.

With the introduction of the new compression index λ into the proposed model, the compression curve and the critical state line are unified. Variation of the compressibility of coarse granular soil with the void ratio and effective pressure can be taken into account, so that the effect of grain crushing on material properties can be captured. Furthermore, the parameters for the compression curve are omitted, so the proposed model can be expressed in a more concise form.

4.4. Plastic Modulus. In the original PZC model, the plastic modulus number H_0 is defined as a constant. Detailed investigations [26] show, however, that the plastic modulus number H_0 changes with the void ratio e. Motivated by the more sophisticated relationships by Ling et al. [21] and by Manzanal et al. [22], the following equation for the plastic modulus number H_0 is used:

$$H_0 = H_0' \exp\left(-h_0 \psi\right), \tag{17}$$

where h_0 and H_0' are the material parameters.

However, Equation (17) cannot reflect the influence of particle breakage on the mechanical behavior for coarse granular soil; therefore, the compression index λ in Equation (16) is introduced. The modified initial modulus is expressed as

$$H_0 = \frac{1 + e_0}{\lambda - \kappa}, \tag{18}$$

where κ is the material parameter.

The modification of the plastic coefficient $H_v + H_s$ is relatively simple. Just remove H_s and turn H_v into a function of the state parameter ψ. Based on the modification of H_v by Manzanal et al. [27], the improved plastic coefficient $H_v + H_s$ is expressed as

$$\begin{aligned} H_v + H_s &= 1 - \frac{\eta}{M_v}, \\ M_v &= M_g \exp\left(-m_v \psi\right), \end{aligned} \tag{19}$$

where m_v is a material parameter, and it remains positive.

For coarse granular soil in a dense condition, the state parameter ψ is negative and M_v is greater than M_g. Thus, this condition where the stress ratio η is greater than M_g will occur, and H_v is positive. As the volume dilates, the void ratio increases, the state parameter ψ gradually tends to zero, M_v decreases, and the peak strength is attained. After that, H_v becomes negative; i.e., the soil behaves in the way of strain softening. Finally, the residual strength is attained. The modification above covers the function of H_s in the original model, so H_s could be reduced.

5. Calibration and Validation

5.1. Calibration. The proposed enhanced model contains 12 parameters, all of which can be obtained from the conventional triaxial test and isotropic compression test, as given in Table 1. The detailed determinations of each parameter are as follows:

Parameters a, b, and c of the enhanced critical state curve can be obtained by fitting the experimental data to Equation (4) through an optimization procedure, where the intercept and the slope of the fitting line are $\ln(a)$ and b, respectively.

The shear modulus number G_0 and bulk modulus number K_0 can be calibrated from the $q-\varepsilon_s$ and $p-\varepsilon_v$ curves of the triaxial compression test, respectively.

Parameters M_g, M_f, m_g, ζ_0, and n which are related to the plastic potential surface and the loading surface can be obtained from the drained and undrained triaxial test. M_g is the slope of critical state line which can be obtained from the $q-p'$ curve of the undrained triaxial test; M_f can be estimated from the relation $M_f/M_g = D_r$; and m_g, ζ_0, and n can be obtained by fitting Equation (14) in which η is the stress ratio of each phase transformation point.

Parameter κ, which is related to the plastic modulus for loading, can be calibrated by the isotropic compression test and the unloading section of the unloading test, corresponding to the slope of the unloading section.

5.2. Validation. For the validation of particle breakage of the proposed enhanced model, the numerical simulation of a series of triaxial compression tests is carried out to compare with the corresponding experimental data obtained from large-scale triaxial tests by Chen et al. [8] for two types of coarse granular soils. The parameters of soils are listed in Table 2, where coarse granular soil I is fresh sandy gravel, and coarse granular soil II is a mixture of weak weathered slate and sandstone. As shown in Table 2, the solid hardness of soil II $h_s = p_a/b^{1/c}$ is obviously lower than that of soil I, which indicates that particle breakage is easier to occur for the mixture of weak weathered slate and sandstone (soil II).

In order to illustrate the superiority of introducing the compression index λ in Equation (18), Equation (17) is alternatively introduced to the enhanced model for comparison. For coarse granular soil I, parameters H_0' and h_0 are 2000 and 5, respectively; for soil II, H_0' and h_0 are 1300 and 2, respectively, and the rest parameters are the same in Table 2 for numerical simulation.

Figure 4 shows the change of the compression index λ under different confining pressures for coarse granular soils I and II, and Figure 5 shows the corresponding variation rate of the compression index λ. For the same coarse granular soil, the greater the confining pressure is, the greater the compression index is, which indicates that the compressibility of coarse granular soil is bigger under higher confining pressure. As shown in Figure 4, with increasing axial strain, the compression index λ firstly increases significantly, and then, the variation slows down, and finally, the compression index λ gradually tends to be stable. This is mainly because that the particle breakage of coarse granular soil occurs under high confining pressure, and the original pores are quickly filled with crushed particles. Correspondingly, the increase of the compression index of coarse granular soil will result in the decrease of void ratio. As shown in Figure 5, the variation rate of the compression index λ reflects the breakage rate of coarse granular particles. The initial variation rate of the compression curve of coarse granular soil II is higher than that of coarse granular soil I under the same confining pressure, which indicates that particle breakage is prone to occur for coarse granular soil II.

Figure 6 illustrates the comparison between experimental data and the numerical prediction for coarse granular soils I and II using the enhanced model by introducing Equation (17).

Under high confining pressure of 2000 kPa and 3000 kPa, both soil samples exhibit similar stress and deformation behaviors. That is, with increasing axial strain, both indicate strain hardening and volume contraction. However, under low confining pressure of 800 kPa, the samples show different mechanical behaviors. With increasing axial strain, coarse granular soil I shows slight softening and significant volume dilation, whereas coarse granular soil II shows continuous hardening and slight volume dilation. From the aspect of particle breakage, under high confining pressure (2000 kPa and 3000 kPa), significant particle breakage occurs for both types of soil, and it inhibits the dilatancy of particles, resulting in strain hardening and volume contraction. Under low confining pressure of 800 kPa, however, different degrees of particle breakage occur for coarse granular soils I and II. As mentioned above, particle breakage is easy to occur for coarse granular soil II (a mixture of weak weathered slate and sandstone) under the same confining pressure. Higher particle breakage inhibits the dilatancy, so that coarse granular soil II also shows strain hardening even under lower confining pressure, and the dilatancy is obviously lower than that of coarse granular soil I.

As shown in Figure 6, the enhanced model by introducing Equation (17) cannot well reflect the inhibition of particle breakage on dilatancy of the soil. Model prediction of deviatoric stress for both samples basically fits the experimental data, whereas without considering the effect of particle breakage, model prediction of volume strain deviates quite far from experimental data. Under low confining pressure (800 kPa), the prediction of dilation grows faster than that expected, while under high confining pressure (2000 kPa and 3000 kPa), the prediction of contraction is insufficient.

In contrast to Figure 6, Figure 7 illustrates the comparison between experimental data and the numerical

Table 1: Parameters and related tests of the enhanced model.

Parameter type	Parameter	Method
Critical state	a, b, and c	Conventional triaxial test or isotropic compression test
Nonlinear elastic	G_0 and K_0	Conventional triaxial test
Plastic flow direction and loading direction	M_g, M_f, m_g, ζ_0, and n	Conventional triaxial test
Plastic modulus	m_v and κ	Isotropic or uniaxial test and unloading test

Table 2: Parameters of the enhanced model for coarse granular soils I and II.

Soil	G_0	K_0	M_g	M_f	m_v	m_g	a	b	c	κ	ζ_0	n
Coarse granular soil I	60	160	1.7	1.5	1.5	0.1	0.36	0.04	0.65	0. 00534	1.5	1.1
Coarse granular soil II	80	80	1.65	1.5	0.2	0.1	0.35	0.03	0.8	0.00194	1.5	1.1

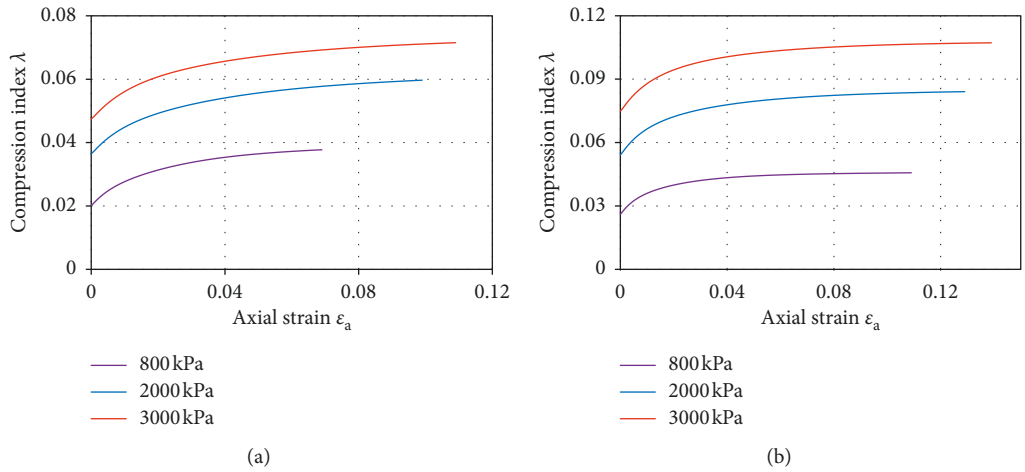

Figure 4: Compression index versus axial strain: (a) coarse granular soil I; (b) coarse granular soil II.

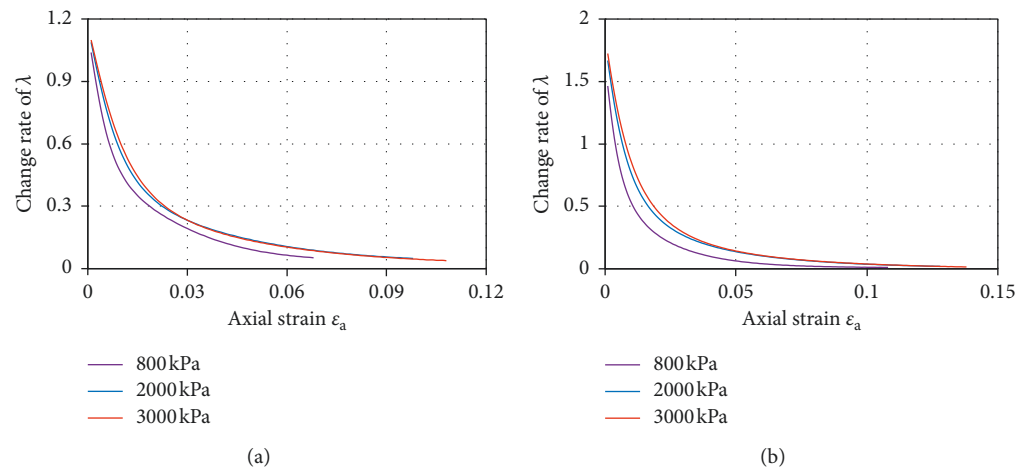

Figure 5: Variation rate of the compression index versus axial strain: (a) coarse granular soil I; (b) coarse granular soil II.

prediction for coarse granular soils I and II using the enhanced model under different confining pressures.

As shown in Figure 7, the modified PZC generalized plasticity model by introducing the compression index λ can well describe the influence of particle breakage on the stress and deformation more accurately for both coarse granular soils I and II. Particle breakage inhibits the dilatancy of coarse granular soil. Model prediction of deviatoric stress in Figure 7 is smaller and fits experimental data better than that in Figure 6, indicating the effect of particle breakage on

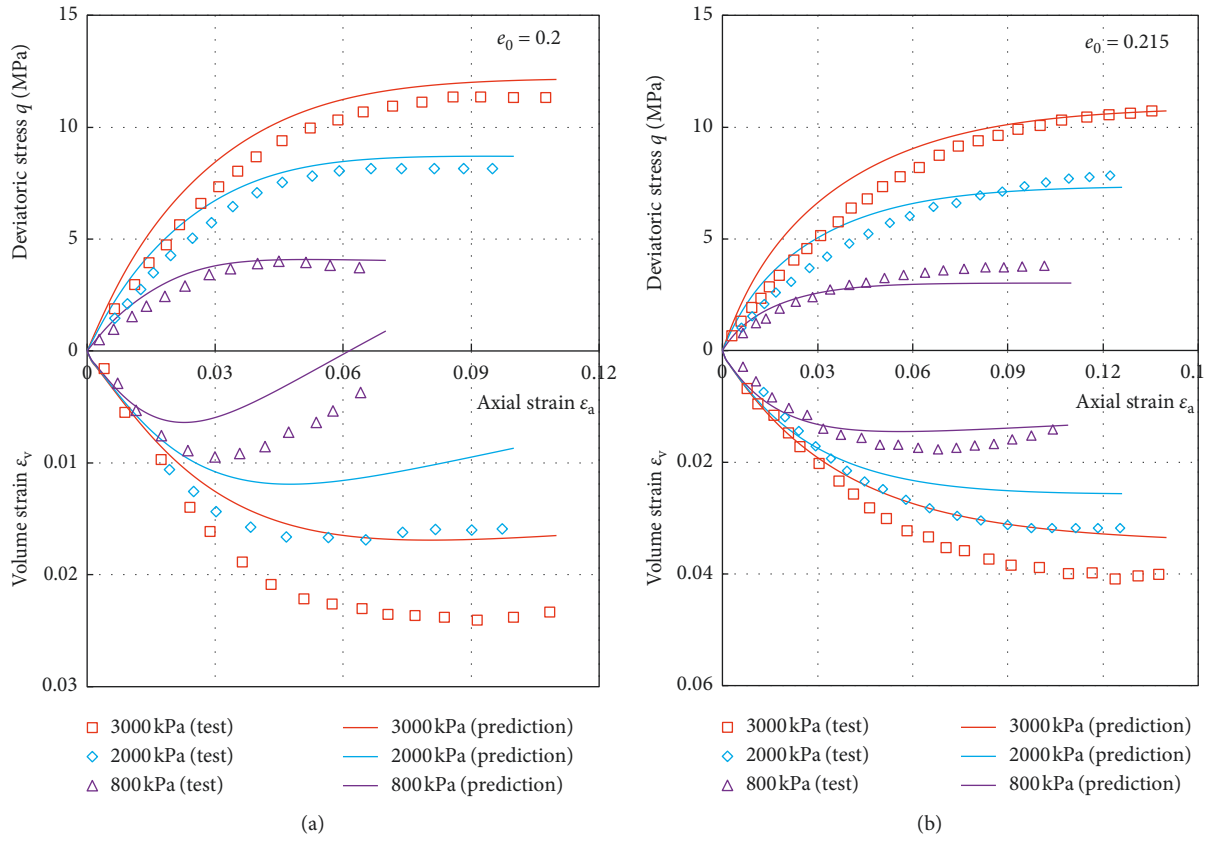

Figure 6: Experimental data and numerical predictions of the enhanced model by introducing Equation (17): (a) coarse granular soil I; (b) coarse granular soil II.

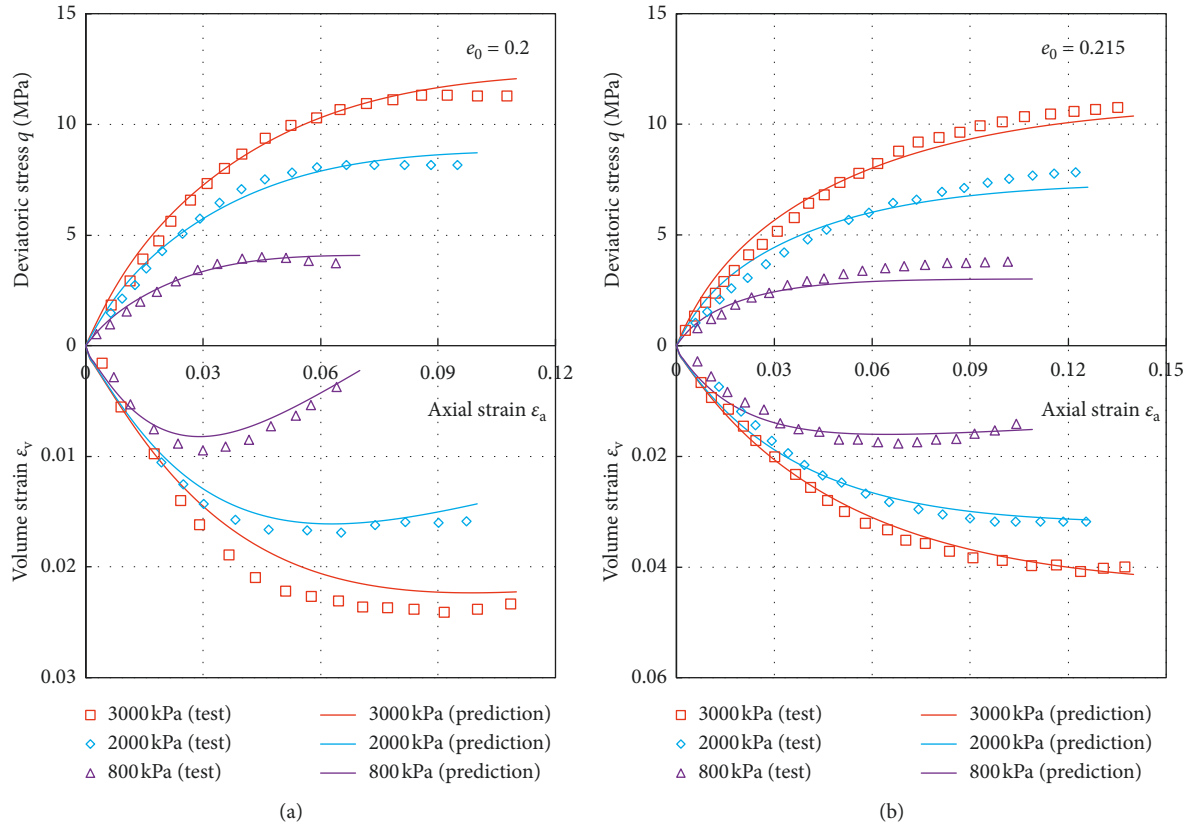

Figure 7: Experimental data and numerical predictions of the enhanced model by introducing Equation (18): (a) coarse granular soil I; (b) coarse granular soil II.

strain hardening of the samples. In addition, under low confining pressure, the prediction of dilation using the enhanced model by introducing the compression index λ decreases significantly, while under high confining pressure, the prediction of contraction increases significantly. The comparison between numerical simulation results with experimental data shows a good agreement, which clearly proves the necessity and accuracy of introducing the compression index λ.

6. Conclusions

Based on the theory of critical state soil mechanics, the compression curve and the critical state line were unified. The present study proposed an enhanced generalized plasticity model for coarse granular soil considering particle breakage within the framework of generalized plasticity. The proposed model has the following characteristics:

(i) Particle breakage is considered by introducing the compression index into the plastic modulus.

(ii) The compression index indicates the compressibility of coarse granular soil and is positively correlated with the confining pressure.

(iii) The change rate of the compression index shows the degree of particle breakage. The more sharply the compression index changes, the more significant the particle breakage is, and vice versa. When the compression index tends to be constant, the particle breakage does not occur any more.

The performance of the enhanced model was validated by comparing the numerical simulation of a series of triaxial tests for two types of coarse granular soils with the experimental data, and good agreement was obtained for both soils. With the good simulating results when applied to monotonic loading, cyclic loading will be considered as well in the next step.

Data Availability

The data used to support the findings of this study are available from the corresponding author upon request.

Conflicts of Interest

The authors declare that there are no conflicts of interest regarding the publication of this paper.

Acknowledgments

This work was supported by CRSRI Open Research Program (Grant nos. CKWV2016376/KY and CKWV2012307/KY), National Natural Science Foundation of China (Grant no. 51009055), and Priority Academic Program Development of Jiangsu Higher Education Institutions.

References

[1] A. R. Russell and N. Khalili, "A bounding surface plasticity model for sands exhibiting particle crushing," *Canadian Geotechnical Journal*, vol. 41, no. 6, pp. 1179–1192, 2004.

[2] W. Salim and B. Indraratna, "A new elastoplastic constitutive model for coarse granular aggregates incorporating particle breakage," *Canadian Geotechnical Journal*, vol. 41, no. 4, pp. 657–671, 2004.

[3] J. A. Fernández-Merodo, R. Tamagnini, M. Pastor, and P. Mira, "Modelling damage with generalized plasticity," *Rivista Italiana di Geotecnica*, vol. 4, pp. 32–42, 2005.

[4] Z. K. Mi, G. Y. Li, and T. L. Chen, "Constitutive model for rockfill material considering grain crushing," *Chinese Journal of Geotechnical Engineering*, vol. 29, no. 12, pp. 1865–1869, 2007, in Chinese.

[5] D. A. Sun, W. X. Huang, D. C. Sheng, and H. Yamamoto, "An elastoplastic model for granular materials exhibiting particle crushing," *Key Engineering Materials*, vol. 340-341, pp. 1273–1278, 2007.

[6] Y. P. Yao, H. Yamamoto, and N. D. Wang, "Constitutive model considering sand crushing," *Soils and Foundations*, vol. 48, no. 4, pp. 603–608, 2008.

[7] E. L. Liu, S. S. Chen, G. Y. Li, and Q. M. Zhong, "Critical state of rockfill materials and a constitutive model considering grain crushing," *Rock and Soil Mechanics*, vol. 32, no. 2, pp. 148–154, 2011.

[8] S. S. Chen, Z. Z. Fu, and H. Q. Han, "An elastoplastic model for rockfill materials considering particle breakage," *Chinese Journal of Geotechnical Engineering*, vol. 10, pp. 1489–1495, 2011, in Chinese.

[9] K. Been and M. G. Jefferies, "State parameter for sands," *International Journal of Rock Mechanics and Mining Sciences and Geomechanics Abstracts*, vol. 22, no. 6, p. 198, 1985.

[10] D. M. Wood, *Soil Behaviour and Critical State Soil Mechanics*, Cambridge University Press, London, UK, 1990.

[11] X. S. Li, Y. F. Dafalias, and Z. L. Wang, "State-dependent dilatancy in critical-state constitutive modelling of sand," *Canadian Geotechnical Journal*, vol. 36, no. 4, pp. 599–611, 1999.

[12] W. J. Cen, J. R. Luo, E. Bauer, and W. D. Zhang, "Generalized plasticity model for sand with enhanced state parameters," *Journal of Engineering Mechanics*, vol. 144, no. 12, article 04018108, 2018.

[13] R. Verdugo and K. Ishihara, "The steady state of sandy soils," *Soils and Foundations*, vol. 36, no. 2, pp. 81–91, 1996.

[14] Z. Mroz and O. C. Zienkiewicz, "Uniform formulation of constitutive equations for clays and sands," *Mechanics of Engineering Materials*, vol. 12, pp. 415–449, 1984.

[15] O. C. Zienkiewicz, K. H. Leung, and M. Pastor, "Simple model for transient soil loading in earthquake analysis I: basic model and its application," *International Journal for Numerical and Analytical Methods in Geomechanics*, vol. 9, no. 5, pp. 453–476, 1985.

[16] M. Pastor, O. C. Zienkiewicz, and K. H. Leung, "Simple model for transient soil loading in earthquake analysis. II. Non-associative models for sands," *International Journal for Numerical and Analytical Methods in Geomechanics*, vol. 9, no. 5, pp. 477–498, 1985.

[17] M. Pastor, O. C. Zienkiewicz, and A. H. Chan, "Generalized plasticity and the modeling of soil behavior," *International Journal for Numerical and Analytical Methods in Geomechanics*, vol. 14, no. 3, pp. 151–190, 1990.

[18] O. C. Zienkiewicz, *Computational Geomechanics with Special Reference to Earthquake Engineering*, John Wiley, Hoboken, NJ, USA, 1999.

[19] F. E. Richart, J. R. Hall, and R. D. Woods, *Vibrations of Soils and Foundations, International Series in Theoretical and Applied Mechanics*, Prentice-Hall, Englewood Cliffs, NJ, USA, 1970.

[20] Z. J. Wang, S. S. Chen, and Z. Z. Fu, "Dilatancy behaviors and generalized plasticity constitutive model of rockfill materials," *Rock and Soil Mechanics*, vol. 36, no. 7, pp. 1931–1938, 2015.

[21] H. I. Ling and S. Yang, "Unified sand model based on the critical state and generalized plasticity," *Journal of Engineering Mechanics*, vol. 132, no. 12, pp. 1380–1391, 2006.

[22] D. Manzanal, J. A. F. Merodo, and M. Pastor, "Generalized plasticity state parameter-based model for saturated and unsaturated soils Part I: saturated state," *International Journal for Numerical and Analytical Methods in Geomechanics*, vol. 35, no. 12, pp. 1347–1362, 2010.

[23] M. C. Liu, Y. F. Gao, and H. L. Liu, "Study on shear dilatancy behaviors of rockfills in large-scale triaxial tests," *Chinese Journal of Geotechnical Engineering*, vol. 2, pp. 205–211, 2008, in Chinese.

[24] E. Bauer, "Calibration of a comprehensive hypoplastic model for granular materials," *Soils and Foundations*, vol. 36, no. 1, pp. 13–26, 1996.

[25] E. Bauer, "Hypoplastic modelling of moisture-sensitive weathered rockfill materials," *Acta Geotechnica*, vol. 4, no. 4, pp. 261–272, 2009.

[26] M. Jefferies and K. Been, "Implications for critical state theory from isotropic compression of sand," *Géotechnique*, vol. 50, no. 4, pp. 419–429, 2000.

[27] D. Manzanal, M. Pastor, and J. A. F. Merodo, "Generalized plasticity state parameter-based model for saturated and unsaturated soils part II: unsaturated soil modeling," *International Journal for Numerical and Analytical Methods in Geomechanics*, vol. 35, no. 18, pp. 1899–1917, 2011.